ANATOMICAL AND FUNCTIONAL ASSESSMENT OF PATENCY OF THE UPPER RESPIRATORY TRACT IN SELECTED RESPIRATORY DISORDERS – Part 1

Andrzej Kukwa[1], Andrzej Zając[2], Robert Barański[3], Szymon Nitkiewicz[4,5], Wojciech Kukwa[6], Edyta Zomkowska[7], Adam Rybak[8]

1) *University of Warmia and Mazury, Olsztyn, Department and Clinic of Otorhinolaryngology, Head and Neck Diseases, Collegium Medicum, Warszawska St. 30, 10-082 Olsztyn, Poland (andrzejkukwa41@gmail.com)*
2) *Military University of Technology, Warsaw, Institute of Optoelectronics, Kaliskiego St., 2, 00-908, Warsaw, Poland (andrzej.zajac@wat.edu.pl)*
3) *AGH University of Science and Technology in Kraków, Department of Mechanics and Vibroacoustics, Mickiewicza St. 30, 30-059 Kraków, Poland (robertb@agh.edu.pl)*
4) *University of Warmia and Mazury in Olsztyn, Department of Mechatronics, Faculty of Technical Science, Oczapowskiego St. 2, Olsztyn, Poland (szymon.nitkiewicz@gmail.com)*
5) *University of Warmia and Mazury in Olsztyn, Department of Neurosurgery, School of Medicine, Oczapowskiego St. 2, Olsztyn, Poland*
6) *Medical University of Warsaw, Warsaw, Faculty of Dental Medicine, Żwirki i Wigury St. 61, 02-091 Warsaw, Poland (wojciechkukwa@gmail.com)*
7) *University Hospital in Olsztyn, Clinic of Otorhinolaryngology, Head and Neck Surgery, Warszawska St. 30, 10-082 Olsztyn, Poland (ezomkowska14@gmail.com)*
8) *LABSOFT Sp. z o. o., Puławska St. 469, 02-844 Warsaw, Poland (✉ adam.rybak3@gmail.pl, +48 501 651 802)*

Abstract

The rapidly developing measurement techniques and emerging new physical methods are frequently used in otolaryngological diagnostics. A wide range of applied diagnostic methods constituted the basis for the review study aimed at presenting selected modern diagnostic methods and achieved diagnostic results to a wider group of users. In this part, the methods based on measuring the respiratory parameters of patients were analysed. Respiration is the most important and necessary action to support life and its effective duration. It is an actual gas exchange in the respiratory system consisting of removing CO_2 and supplying O_2. Gas exchange occurs in the alveoli, and an efficient respiratory tract allows for effective ventilation. The disruption in the work of the respiratory system leads to measurable disturbances in blood saturation and, consequently, hypoxia. Frequent, even short-term, recurrent hypoxia in any part of the body leads to multiple complications. This process is largely related to its duration and the processes that accompany it. The causes of hypoxia resulting from impaired patency of the respiratory tract and/or the absence of neuronal respiratory drive can be divided into the following groups depending on the cause: peripheral, central and/or of mixed origin. Causes of the peripheral form of these disorders are largely due to the impaired patency of the upper and/or lower respiratory tract. Therefore, early diagnosis and location of these disorders can be considered reversible and not a cause of complications. Slow, gradually increasing obstruction of the upper respiratory

tract (URT) is not noticeable and becomes a slow killer. Hypoxic individuals in a large percentage of cases have a shorter life expectancy and, above all, deal with the consequences of hypoxia much sooner.

1. Introduction

The anatomical area covering the *upper respiratory tract* (URT) and the *lower respiratory tract* (LRT) is shown in Fig. 1 [1, 2]. Figure 1 shows graphically the area of LRT (larynx, trachea, bronchi, bronchioles), classically defined area of URT (nose with the nasal cavity and paranasal sinuses, pharynx), and the proposed extension for the purpose of this definition study of the URT area due to the significant convergence of methods of apparatus based diagnostics [3, 4].
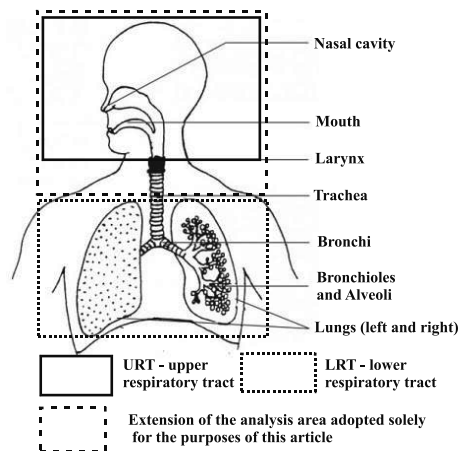

Fig. 1. Schematic representation of anatomical areas covering diagnostic and therapeutic space of otolaryngology.

The basis of effective treatment of respiratory system disorders is modern diagnostics of diseases in clinical practice. When analysing the current possibilities of physical diagnostic methods that can be applied in otolaryngology, it appears that the current state of development of measurement methods allows for very precise quantitative diagnostics and, in selected cases, only qualitative diagnostics. The list of available options within physical sciences (sometimes referred to as medical physics) is shown in Fig. 2. The area of diagnostic methods used, presented in Fig. 2 is very broad, and in a specific area of medical activity (both diagnostic and therapeutic) it is necessary to adjust medical needs to the diagnostic possibilities necessary to perform the tasks of a specific medical centre.

The diagnostic methodologies shown in Fig. 2 have been divided according to the physical phenomena used in a given method, *i.e.*, from the area of optics, acoustics and radiation phenomena with the use of high-energy photons (X-rays in both imaging and tomographic techniques), and phenomena related to the recording of the microwave spectrum, such as *magnetic resonance imaging* (MRI). From the application area indicated in Fig. 2, MRI was distinguished. In terms of the source of the signal, it differs from the methods using X-ray radiation as specified in Fig. 2
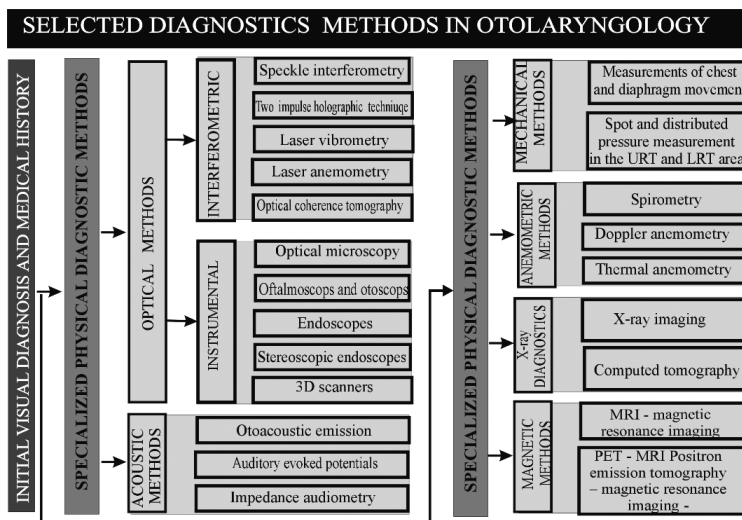
Fig. 2. Selected physical diagnostic methods used in otolaryngology.

and the analysis of its absorption in biological centres. However, in terms of the effect, it is similar to *computed tomography* (CT) for the obtained spatial distribution differentiates tissues and, in the case of MRI, the water content in tissue structures. This is in contrast with CT differentiating tissues in terms of the content of elements with different absorption of X rays (tissues containing elements with higher atomic numbers dampen X-rays more strongly). In the case of MRI, the alternating magnetic field interacts with the magnetic moment vector of atomic nuclei (mainly in hydrogen atoms) as a result of which *electromagnetic radiation* (EM) in the range of radio frequencies recorded by the MRI set is generated, and differentiates tissues with different water content in the detection area of microwave radiation.

It is also necessary to consider the division of the mentioned diagnostics methods in terms of the effect obtained as a result of their application:

- Methods for imaging the surface of the examined organ – photography, microscopy, endoscopy, interferometry, holography, structural light methods,
- Examination of the internal structure – CT, *Optical Coherence Tomography* (OCT) (but in a small range of thickness of the analysed structure), MRI,
- Methods allowing for dynamic tests – anemometry, ultrasound, including those using the Doppler effect (blood flow test), laser anemometry.

2. Analysis of diagnostic needs in the area of examining respiratory disorders

In the present state of medical knowledge, it is obvious that individuals who are hypoxic due to various anatomical and physiological disorders have shorter life expectancy in a large percentage of cases. This also results in the fact that they deal with the medical consequences of hypoxia much sooner. Such consequences (they can, and should be, called complications) manifest themselves in diseases that are difficult to correlate with respiratory disorders, *e.g.*, in the form of:

- hypertension,
- heart diseases,
- early type 2 diabetes,

815

- early pathology of the cerebral vessels, often leading to a stroke,
- many other disease processes: it seems they can even affect the early stages of embryo development.

Respiratory disorders are very often most easily and clearly manifested during sleep. They are then beyond our consciousness, controlled by the *central nervous system* (CNS) which causes that their measurement results correspond to the values of actually existing hypoxia. It is also obvious that during the wakefulness phase one is not always aware of insufficient respiration. Only in the period of much more intense demand for oxidation, *e.g.*, during physical work, can one control the parameters of the respiration process. On the other hand, in the case of impaired patency in the nasal area or in individual sections of the pharynx and even in the lower respiratory tract, the mouth is opened for the expected breathing supplementation. Only a sudden (severe) demand (noticeable hypoxia) makes one aware of the need and the resulting necessity to contact a specialist. However, it is not a known phenomenon that in the case of slowly, gradually increasing obstruction (especially within the URT) that one behaves slightly differently. Patients go to a specialist only when their bed partners are disturbed by loud snoring and often scared by repeated apnoea (periods of complete cessation of breathing, apnoea of very different duration). Patients then begin to feel obliged to undergo diagnostics, medical observation and, finally, treatment.

The classic method of extensive diagnostic tests is encephalography, which has been used in extended diagnostics for several dozen years [5]. The outline of its methodology is shown in Fig. 3 and selected cases of analysis in Fig. 4.
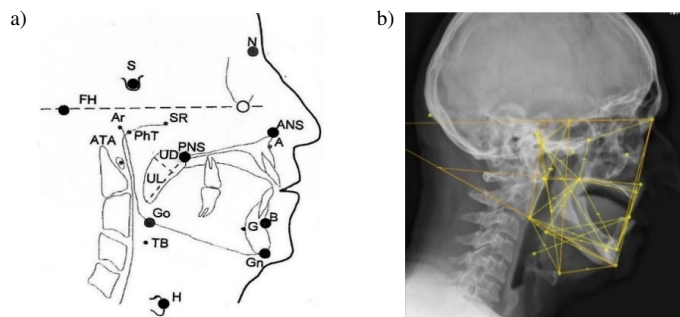

Fig. 3. A visualization the methodology of cephalometry used in otolaryngology. The figure shows: a) the distribution of individual anthropometric points with the view of the lines of individual measurements (dashed sections) and the reference of selected measurement areas to individual anatomical parts of the craniofacial region b), examination view for anatomical assessment of the upper respiratory tract using a computer program written for patients of the Hospital of the University of Warmia and Mazury.
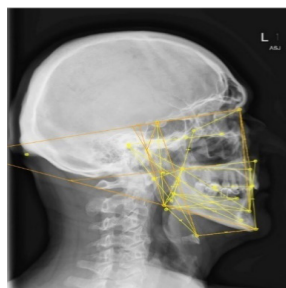

Fig. 4. Examples of cephalometric analysis in two selected cases [6].

Upon analysing the current state of diagnostics and the resulting conditions for treating obstructive respiratory disorders (particularly sleep disorders), many years of stagnation can be seen in both these areas. Due to the noticeable lack of significant progress in diagnostics of obstructive sleep apnoea, which also significantly affects detection, and especially treatment of this disease, there is a need to develop adequate methods and instrumentation. A preferably relatively cheap method, simple in application for a detailed assessment of respiratory tract patency, detection of anatomical changes in the URT, and diagnostics of the level of inconvenience caused by obstructive respiratory disorders during sleep should be quickly implement into medical practice. The existing anatomical and functional conditions must also be taken into account.

Among the possible methods for anatomical assessment of the URT before and after surgical treatment, in the majority of cases, the most important examination is cephalometry and laryngological examination with the use of endoscopy. For cephalometry, in many cases, the evaluation of parameters comes down to a cursory visual assessment of the X-ray image, while in more complex cases, CT or, recently, also *Spiral Computed Tomography* (SCT). Due to the costs of purchasing and operating a CT (SCT) device, this methodology is currently used only by larger medical centres. However, it should be remembered that, regardless of the diagnostic capabilities of a physician, it is always particularly important to pay attention to the patency within the nasal cavities, nasopharynx and other parts of the pharynx down to the glottis.

In the presented study, the authors show and discuss the proposed methods of URT examination, using a newly developed method. The said method was developed [7–9] and tested in outpatient conditions, involving a set of two devices and dedicated software for the analysis of diagnostic data (both qualitative and quantitative in selected cases) to assess airflow through the URT (Fig. 3). These issues (the improvement of the qualitative and quantitative detection of existing functional or anatomical disorders) were also addressed in the developed software for quantitative analysis of the results of the examination with the use of SCT [7].

Examplary results (both qualitative and quantitative) of the analysis of the size of air passages in the area of the patient's head (the measurements are based on the SCT examination) are shown in Fig. 3 [7].

The measurement results presented in Fig. 5 do not allow for quantitative assessment of the airflow through the respiratory passages, providing only the size of the passage cross-sections at selected points in the respiratory tract. The program used for the analysis and visualisation of
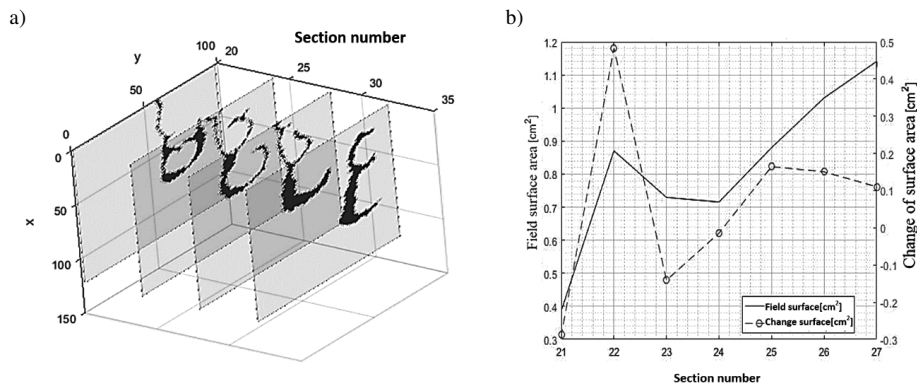

Fig. 5. Examples of results of quantitative measurements of the air passages' cross-sections of the facial skeleton of an NN patient. Graphs derived from standard SCT results. Figure a) presents a visualisation of the area of subsequent cross-sections of the air passages and sinus chambers; Figure b) shows a graph of these quantities in numerical values – surface area in selected cross-sections and the rate of changes in the cross-section area of the air passages.

CT (SCT) measurement results was developed by the authors of this study and written in Matlab using the Image Processing toolbox. A developed graphical user interface was used to control the program. In order to simplify the operation, the main program window has been divided into sections. Each section is responsible for a certain stage of program operation, and each of them (in a certain logical sequence resulting from the detailed structure of the algorithm built) can be separately initiated to obtain the desired parameters of the assessed cranium space.

In addition to determining the geometry of the URT air passages using the above-mentioned method, it is also possible to quickly and precisely measure the values of air flows within the URT. As regards the measurement of the volume/rate/stream of airflow through the respiratory passages in the URT area, new measurement methods should be of primary importance. Creating a new group of miniature flow and pressure sensors allows for new designs of devices to analyse flows and pressure within the respiratory passages. One of the proposals is an instrument specially developed, built and tested for such measurements. The use of the device patented by the authors, *i.e.* the NasoOroSpirometer, (Fig. 6) allows, among others, measuring:

- airflow rates through individual respiratory passages – both nasal passages independently,
- oral flow rates,
- inspiration and expiration volumes,
- characteristic times of inspiration, expiration and apnoea,
- calculation (a program to analyse parameters of the respiratory cycle developed for the device) of many other parameters – *e.g.*, symmetry of the flow through the nasal passages.

Thanks to a specially designed mask (the shape of which is individually adjusted and made for each patient in the form of a flexible, disposable filling element of a rigid mask – Fig. 7), it is easy to obtain measurements by carrying out diagnostics of selected disorders. The implementation of an individual fitting element takes approximately five minutes, which slightly extends the examination time.

It should be assumed that both imaging (X-ray, CT [SCT] and MRI) results as well as selected physical examinations (measurements of gas flow through measurement passages, pressure tests inside the body cavities, endoscopic examinations and similar) can demonstrate respiratory disorders and can be collected in the proposed URT diagnostic procedure.

The objective of the implementation of the discussed diagnostic and measuring devices is to help determine the causes and dynamics of impaired ventilation, both in the period of full awareness and physical activity and during sleep. The possibility of objectively assessing and visualising URT disorders helps explain disorders to patients, the advisability of correcting the impaired patency of the URT and the spectrum of symptoms accompanying such disorders.

One should strive to define only the scope of examinations which (due to sequence of their implementation) allow for anatomical and functional assessment of the URT. This will allow, first of all, to mark the location of the existing obstruction and, using cephalometry, it will be possible to mark the location of the obstruction revealed during respiration with great accuracy, initially in the form of a breathing noise and then in the form of snoring during sleep. At the same time, depending on the size of the obstruction, the patient will supplement nasal respiration (supporting) with oral respiration to a different degree. This results, as noted, in shifting the pattern of breathing from nasal to oral.

It is also worth recalling a frequently used diagnostic method, *i.e.*, endoscopy. The endoscope is a speculum typically containing an optical image guide [10], additionally equipped with an illuminator system. In the current state of the art, lighting is provided with *light-emitting diode* (LED) sources. While maintaining the functionality of lighting with LED sources, it has recently become possible to use a miniature *complementary metal–oxide–semiconductor* (CMOS) camera system instead of an image guide. The use of modern lighting technologies – both in the image
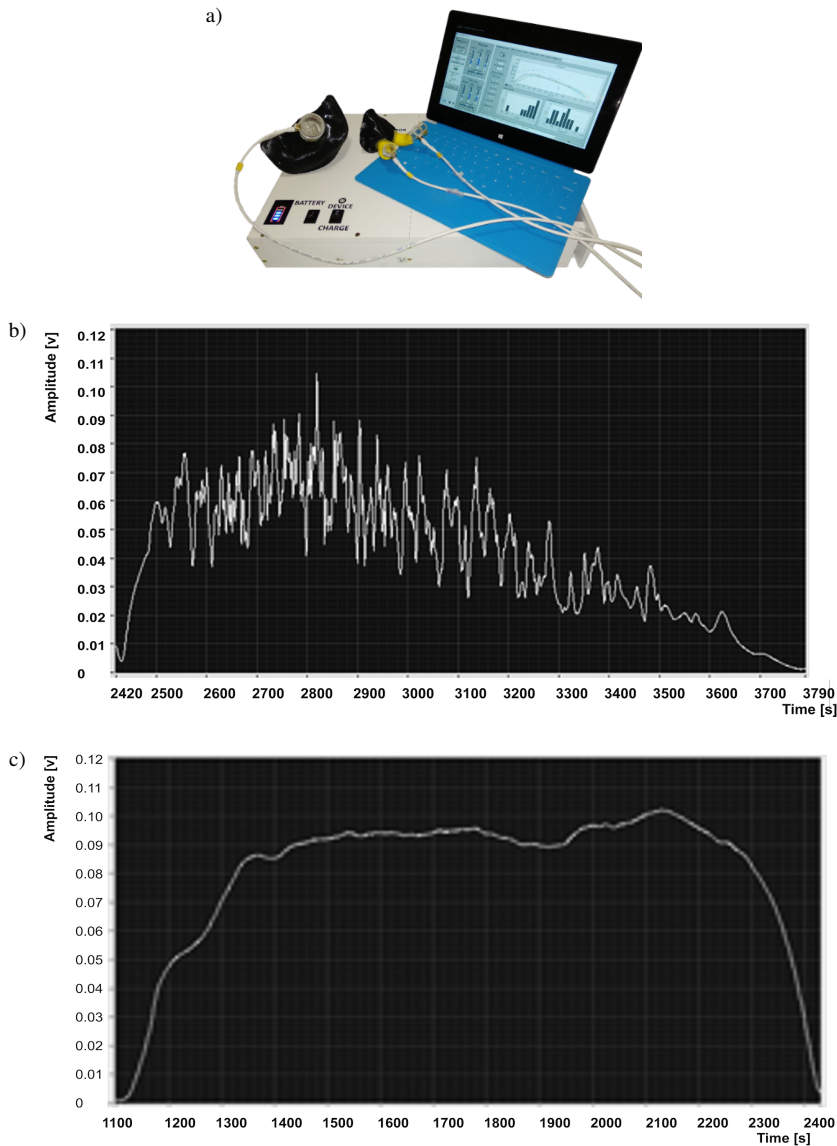
a)

b)

c)

Fig. 6. The NasoOroSpirometer set a) developed by the authors of the publication, and examples of the recorded flow during inspiration b) and expiration c). The visible, rapidly changing flow signal during expiration results from the physical impact of micro-drops of water vapour in the expired air – it has humidity close to 100%, while inspired air humidity fluctuates around 50%. Figure a) shows: the measurement unit (grey), elements of the measurement mask (black) and a palmtop with installed software for visualisation and analysis of measurement results. The presented system has been patented – P.419511.

guide system and in the CMOS camera system, allows for additional effects related to adjusting the colour temperature of the light source obtained in such a modern illuminator. This allows for the use of colour contrast highlighting the details of the observed organ [11, 12]. Its basic functionality is used to examine organs from the outside, when they are accessible through
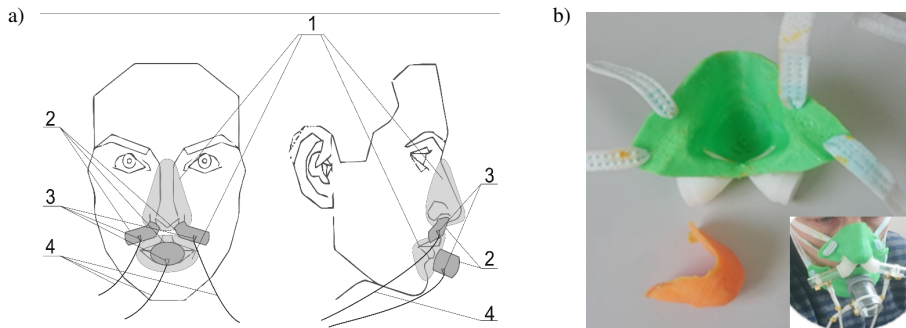
Fig. 7. Measuring mask to analyse the airflow in the measurement of the respiration process. Figure a) presents a diagram of the arrangement of the mask measurement elements: 1 – the mask supporting structure, 2 – structural elements for the assembly of thermal anemometer sensors (or semiconductor sensors), 3 – flow sensors for the analysis of ventilation through the nasal passages (two identical sensors for each independent passage measurement for each) and the mouth, 4 – electric signal transmission paths to the measuring unit – shown in Fig. Figure b) shows the structure of the mask – green indicates the main part of the mask made in the same version (three basic sizes) for a certain group of patients, orange indicates individual, disposable sealing insert, the lower right corner of the picture shows the assembled diagnostic mask.

the natural openings and canals of the body. Unlike other medical imaging techniques, the endoscope probe is inserted directly into the body canal. Such a procedure is often uncomfortable for the patient, *e.g.*, colposcopy or urinary tract examination; however, some procedures in otolaryngology are less discomforting. Endoscopy is a diagnostic and medical procedure used to detect pathological changes and, if necessary, to perform a biopsy to collect material for histopathological examination. The assessment of the absolute scope of pathological changes using an endoscope requires experience from the operator. Stereovision endoscopy extends the structure of the endoscope with a second lens, making binocular stereoscopic observation possible. The second lens is on the same surface as the first lens and is only offset from the first one. The disadvantage of this solution is the larger diameter of the endoscope, which may limit its use. Structured light endoscopy expands the endoscope with a pattern generator of this type of light. The endoscope camera displays the pattern displayed on the surface of the object.

The next presented device is used to measure pressure at four arbitrarily determined levels (places) of the respiratory tract, with the possibility of an application to analyse pressure in the oesophagus (there are significant differences in this area, especially in the case of sleep apnoea). Such tests aim to assess the differences in the resulting pressures within the nose, mouth, nasopharynx and oesophagus. Determining the resulting pressure so that it will reveal its value during sleep, which will lead to a change in the pattern of breathing from the nasal respiration pattern to the oral one. The respiratory drive is then completely under the control of the autonomous system, and it operates regardless of one's will.

3. Selected cases of diagnosed disorders

In this part of the study, selected examples of use of the developed measurement methods and dedicated diagnostic devices with the possibility of using them in otolaryngology will be presented, including the following:
– the examination and device for naso-spirometry,
– the examination and instrumentation for cephalometry,
– endoscopy and its methodology as well as proposed complementary tests.

3.1. Nasal and oral spirometry

The study was based on the classic spirometry technique in the presented solution using the airflow measurements within the URT.

Figures 6 and 7 show the discussed device and the principle of constructing an individual measurement mask. Fig. 8 shows a diagram of the NasoOroSpirometer virtual control panel. The figure shows the main commands that allow users to turn on the various functions of the device and an example of the measurement process: the left nasal passage in white, the right nasal passage in red, the sum of both waveforms in blue. The colours of the waveforms on the screen are entered permanently – the passages are selected using the buttons on the right side of the screen. Other buttons: in the top line BREATH – performs the measurement, the results from connected sensors are saved (maximum three), while the results obtained in the last 20 seconds are visualised on the screen, HISTORY – quick reading of the last 10 minutes of measurements, EKG – ECG waveform (if the electrodes are connected, a simplified two-electrode reading is used), as well as possible saturation (if an oximeter is connected), PATIENT – personal data recording block and a medical interview carried out before the measurement for the patient undergoing the test; after saving the data. (it allows the user to generate a report on the test results), INSTITUTION – data of the centre where the test is carried out, as well as the data of the person performing the test, FILE READ – Reading the entire test file without analysing the test itself, SETTINGS (button on the right upper side of the line) – configuration of the device, passage outputs. In the bottom line of commands there is TEST START – current calibration of the device (if necessary) and starting the measurement, RECORD – recording the test, time [s] – setting the time after which the test is to end (automatically) in the case of "0" – information; next window – a clock indicating the test time that has already elapsed, EXIT – to exit the program. In addition, the indicators applied to the visualisation of the generalised patient's face indicate the approximate dynamics of the measurements being carried out – the colours allow for simple identification of the measurement passages.

Fig. 8. View of the control panel (virtual control panel of the device generated on the control computer screen) of the NasoOroSpirometer.

In its classic version, spirometry is a static measurement of the efficiency of the lower respiratory tract, and only to a small extent and indirectly also for the assessment of the upper respiratory tract. Typical spirometry consists in measuring the physical parameters of oral breathing, omitting the nose and the nasopharynx [13, 14]. The typical course of the examination is to measure the tidal volume and the duration of individual stages of breathing. It also allows for indirect determination of resistance in the respiratory tract, *i.e.*, it mostly reveals resistance in the respiratory system and its condition in the upper part. Spirometry allows for assessing the efficiency of the respiratory system as a whole, with bronchi, bronchioles, lungs and chest mechanics participating in this process.

Standards of the spirometry technique can be divided into two stages. The purpose of the first stage is to measure the so-called vital capacity of the lungs. This consists in measuring (1) the *tidal volume* (referred to as TV) – the amount of air that is inspired and expired during normal breathing, (2) the *inspiratory reserve volume* (IRV) – the amount of air by which normal inspiration can be deepened and (3) the *expiratory reserve volume* (ERV) – the amount of air that can still be "removed" from the lungs by expiring after normal expiration.

In addition to this basic set of respiratory parameters determined in the study, in the next stage of spirometry measurements, it is possible to determine: (1) *forced expiratory volume in the first second* (FEV1) – the amount of air removed from the lungs during the first second of forced expiration, (2) *forced vital capacity* (FVC) – the amount of air removed from the lungs during all forced expiration, (3) the Tiffeneau ratio – the value of this ratio indicates what part of the FVC or VC volume is FEV1, and (4) *peak expiratory flow* (PEF) – the maximum airflow rate through the respiratory tract that was achieved during forced expiration. Schematic physiological parameters of the respiration process obtained in spirometry are shown in Fig. 9.
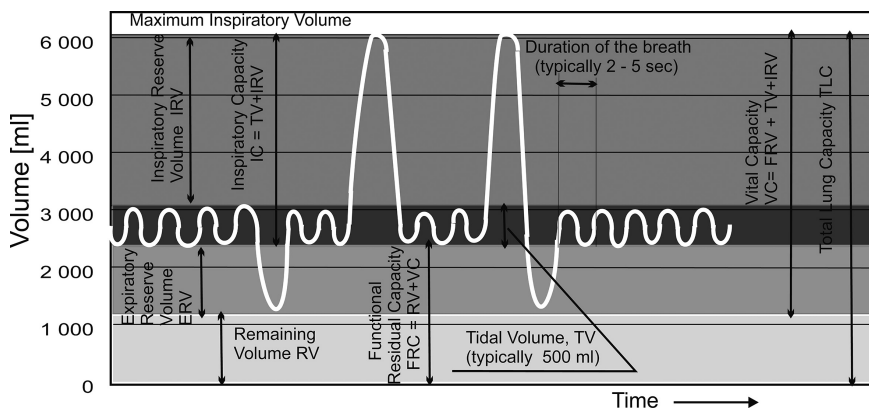

Fig. 9. Diagram of an exemplary, achievable waveform of the respiration process recorded in spirometry. The chart shows a typical area of variability in parameters determined in spirometry tests. The figure describes individual volumetric parameters obtained during the examination and provides their English acronyms. The respiratory parameters presented in Fig. 9 which can be obtained in standard spirometry are defined below.

– *Tidal Volume* (TV) – being the volume of air inspired or expired (during a single inspiration-expiration cycle, it is not the same volume, but during a longer sequence of inspirations and expirations, their average value is the same) during a single calm respiration, during the period of full awareness and sleep, measured in a specified time or converted into a unit of time. In the latter case, it corresponds to the rate of changes in lung gas volume per unit time,

- *Inspiratory Reserve Volume* (IRV) is the largest volume of air that can be additionally drawn into the lungs after the end of calm inspiration – this parameter can also be converted into a time unit and also determines the rate of changes in the volume of air,
- *Expiratory Reserve Volume* (ERV) – the largest volume of air that can be blown out when one expires gently,
- *Inspiratory Capacity* (IC) – the largest volume of air that can be drawn into the lungs after completing gentle inspiration, IC = TV + IRV,
- *Vital Capacity* (VC) – greatest change in lung capacity measured between maximal expiration and maximal inspiration VC = TV + IRV + ERV, the volume of air that can be blown out when expiring gently,
- *Inspiratory Capacity* (IC) – the largest volume of air that can be drawn into the lungs after completing gentle inspiration, IC = TV + IRV,
- *Vital Capacity* (VC) – the largest change in lung capacity, measured between maximum expiration and maximum inspiration, calculated based on VC = TV + IRV + ERV.

In addition to measuring the volume of inspired/expired air, including measuring the rate of individual respiration phases, the times characterising individual phases of the respiratory process were also measured. Currently, spirometry is the only generally available functional measurement of respiratory parameters. This does not apply to specialised tests and measurments and to diagnostic equipment used in competitive sports – *e.g., cardio-pulmonary exercise test* (CPET).

When analysing the metrological parameters of spirometry, it should be noted that the natural route of air passage to and from the lungs is the nasal tract, and spirometry is based on the passage only through the mouth – the patient's nostrils are intentionally closed for the duration of the test (usually with a clamp). One should also consider that spirometry (without involving ventilation disorders in the URT area) is mainly intended to diagnose LRT diseases.

However, it is known that most resistance, especially inspiratory, is found within the URT. Therefore, starting from the anterior nostrils and ending in the glottis area, it should be understood that all deformations in anatomical and functional terms concerning individual components such as the activity of pharyngeal muscles as well as neural supply and coordination will affect the respiratory function, constituting a problem/measure of the emerging obstruction. The encountered disorders may (and will) have a different influence on patency, and thus on the emerging respiratory resistance. That is why it was decided to construct devices to measure the above-mentioned resistance and develop an appropriate algorithm supporting diagnostics and documenting the obtained results.

A simplified diagram of the algorithm developed for the analysis of measurement results is presented in Fig. 10. The proposed measurement procedure allows for the measurement available through all three passages, *i.e.*, oral and two nasal passages, with the possibility to connect both nasal passages or only measuring the flow through the mouth. Before starting the test, it is possible and even necessary to calibrate the device to measure the absolute flow through individual respiratory passages. The calibration procedure does not have to be performed before each measurement, but only when the environmental parameters significantly differ from the laboratory conditions. It is also worth calibrating the device every week or if unusual measurement values are noted. The calibration procedure itself is very simple and requires three single measurements (for each sensor separately) by registering the flow of a given, known volume, *i.e.*, 500 ml of air.

Figure 11 shows an example of a signal waveform obtained from one sensor. The differences in the signal character for three measurement sampling rates – 1 kHz (typical usable recording frequency obtained with a USB-6002 measurement card) and 100 Hz and 10 Hz are shown. Since the typical respiratory frequency ranges from 0.2 to 0.5 Hz, each presented case meets the Nyquist criterion [15]. As can be observed, for each case, both the nature of the waveform and the duration
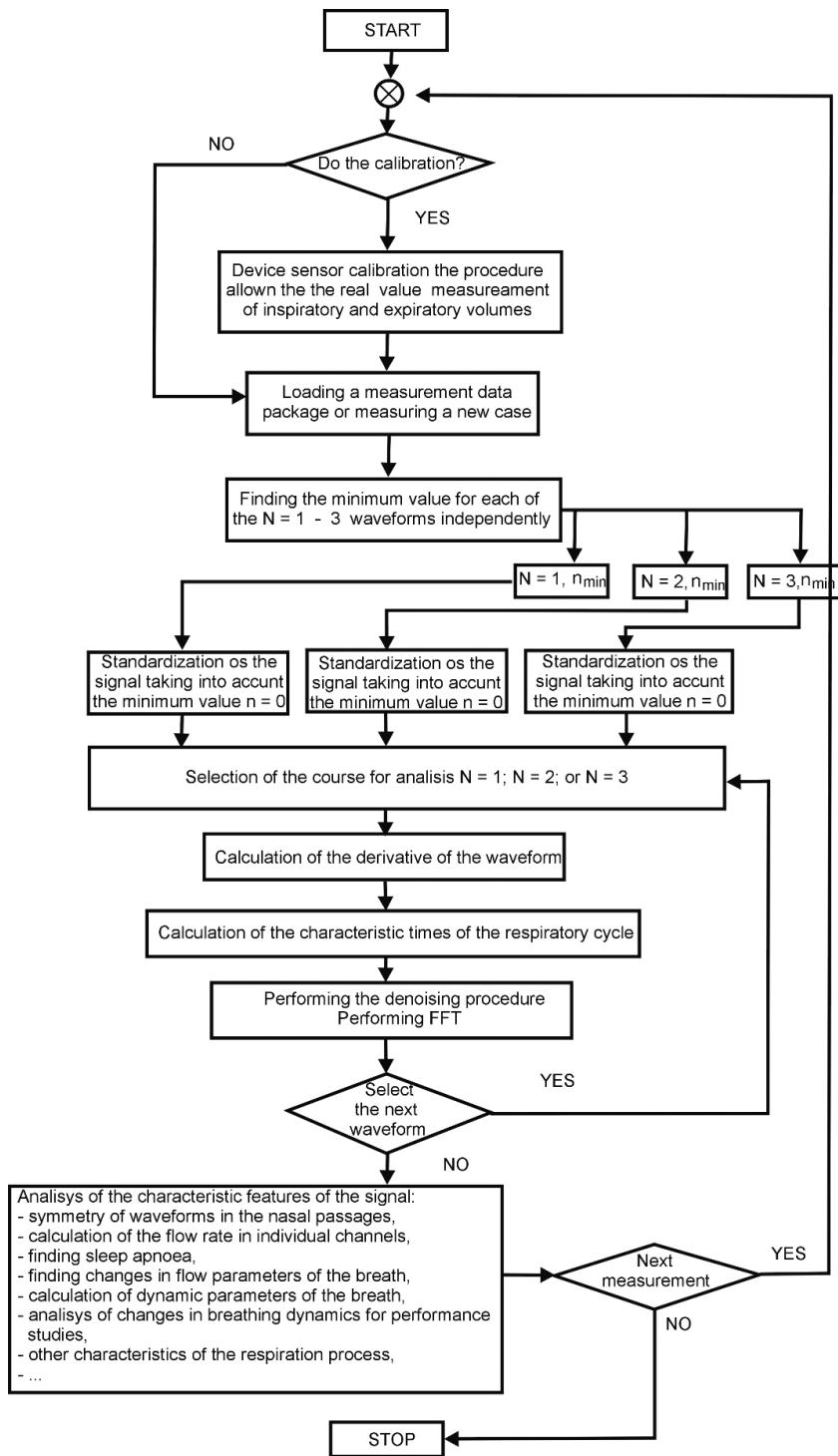
Fig. 10. Algorithm for the measurement and initial analysis of respiratory parameters implemented
with the NasoOroSpirometer.

of individual stages of the respiration process are the same for all the waveforms. This allows for recording a much smaller amount of measurement data without losing the details of the values in the mass memory of the control computer during the measurements, which is particularly important in the implementation of many hours of examinations, *e.g.*, overnight measurements related to the diagnostics of respiratory disorders during sleep.
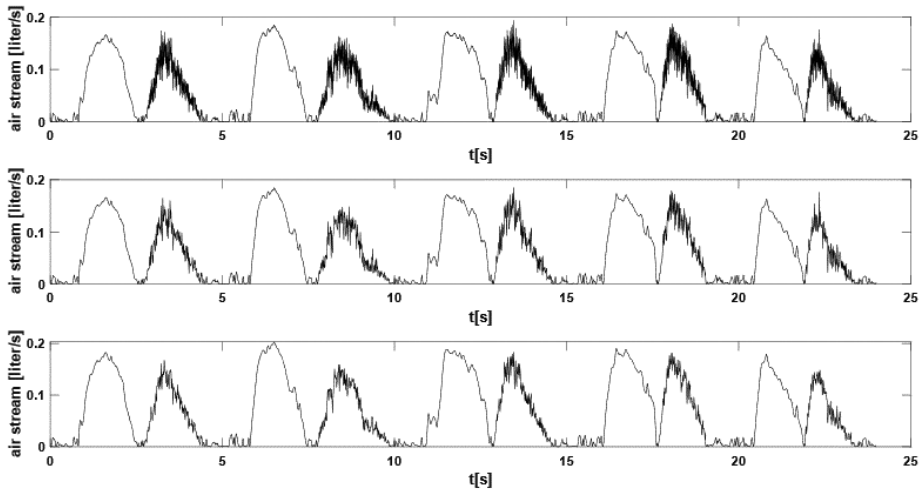

Fig. 11. Example of a signal waveform from the measuring instrument. The figure shows from the top: the waveform obtained at the sampling rate of 1 kHz, at the sampling rate of 100 Hz (middle graph), and the sampling rate of 10 Hz. All waveforms present the results of digital processing of the basic waveform – first from the top – saved by the measurement card of the device. The procedure for obtaining the waveforms consisted in taking from the measurement stream every 10th (middle graph) – or every 100th (bottom graph) – measurement result.

However, it is worth noting that frequencies higher than typical respiratory rates recorded in the signal's waveform's signal can be noted. This is visible in Fig. 12. It is worth considering this problem for a moment.

Figure 12 shows a section of a typical measurement waveform in its upper part – from left to right: inspiration, expiration, and another four such cycles. The difference between the inspiratory phase and the expiratory phase is clearly visible. According to the authors, the difference results from the difference in the physical parameters of the inspired air (typically air at approx. 20°C and humidity in the range of 30–50%) and expired air (typically air at 36.6°C and humidity of approx. 90–95%). There is a reasonable presumption that the applied method of thermo-anemometric measurement using a sensor in the form of a tungsten wire with a diameter of approx. 5 μm heated to a temperature of 200°C is very sensitive to the humidity of the medium flowing around it. When the air is saturated with vapour at a temperature close to condensation temperature, in the air expired from the patient's lungs, there is a mist, which in the case of contact of the microdroplets with the wire will temporarily cool the sensor, which will seemingly increase the measured value.

After the water evaporates, the sensor returns to its original temperature (a thermo-anemometer with a constant measuring temperature of the sensor), which results in oscillations only in the expiration phase. However, it should be noted that the visible oscillations are not related to the measured respiratory flow parameters but are a stochastic process superimposed on a typical thermo-anemometric measurement. A *Fast Fourier Transform* (FFT) analysis indicates a typical
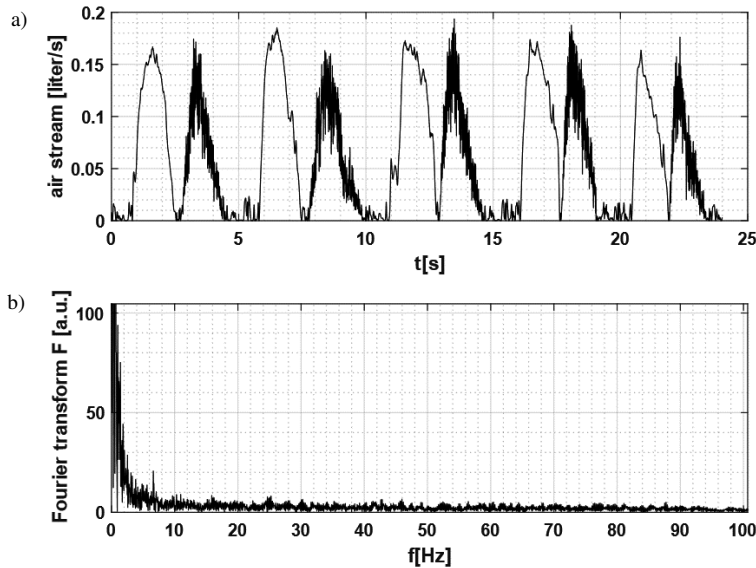
Fig. 12. Selected measurement waveform (a) and Fourier transform of this waveform (b). The lower graph shows the appearance of a typical band for respiration (on the left to the value of about 10 Hz) and in the range 10 – 80 Hz, with a local maximum of about 16 Hz, 25 Hz, 46 Hz and in the range of about 60 – 80 Hz. This indicates the recorded signal of higher frequencies related to thermal fluctuations of the measuring system of the anemometer sensor in the waveform.

fluctuation frequency of approx. 24 Hz (approx. 40 ms). This time can also be estimated from an analysis of thermal properties of the sensor and droplet parameters in the expired water-saturated air – for 100% humidity, the estimated frequency of temperature changes, $i.e.$, visible as having no physical basis, the speed fluctuation is no more (at 100% temperature modulation) than approx. 60–100 Hz. Such an estimate, in which the sensor power supply was not taken into account, significantly affecting the scope and duration of a single fluctuation, is sufficiently consistent with the obtained measurement results.

Since it only occurs during one of the phases of respiration (expiration only), it allows for automatic differentiation of the two phases of respiration – expiration and inspiration. An example of analysis allowing for the differentiation of phases of respiration is presented in Fig. 13. As it can be seen, only during expiration does the derivative assume significant values (above 0.02) and during outside inspiration it is close to 0.02.

The graphs in Fig. 13 show the value of the derivative of the tested signal obtained at different sampling frequencies of the tested signal. Signal fluctuation is particularly visible in the waveform sampled with the frequency of 1 kHz (first graph from the top). In the other cases, due to the non-fulfilment of the Nyquist condition, the effect is visible, but the use of these cases for automatic differentiation of characteristic times in the respiration process is no longer obvious but still possible.

According to the authors, fluctuations in the waveform of measuring the airflow rate through the respiratory tract are caused by the absence of a frequency modulating the signal associated with thermal effects on the sensor surface and result from much higher humidity of expired air outside expiration.

Figure 14 shows examples of results obtained for calculations of the signal derivative value for selected expiration.
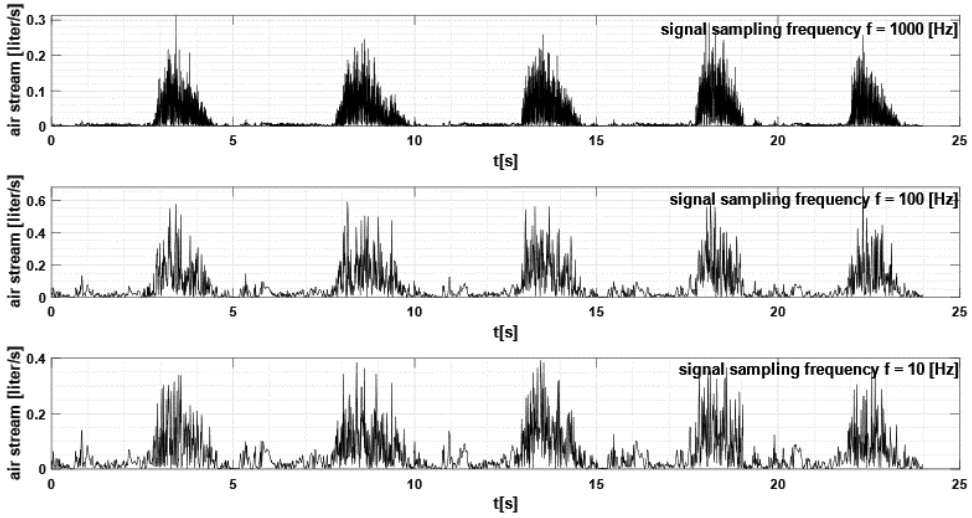
Fig. 13. Calculated derivative module of the waveforms presented in Fig. 11. For comparison, the results of calculations for the same sampling frequencies (1 kHz, 100 Hz and 10 Hz) are shown in sequence at the top of the figure. For easier visualisation, the derivative module divided by 100 is incorporated on the graphs.
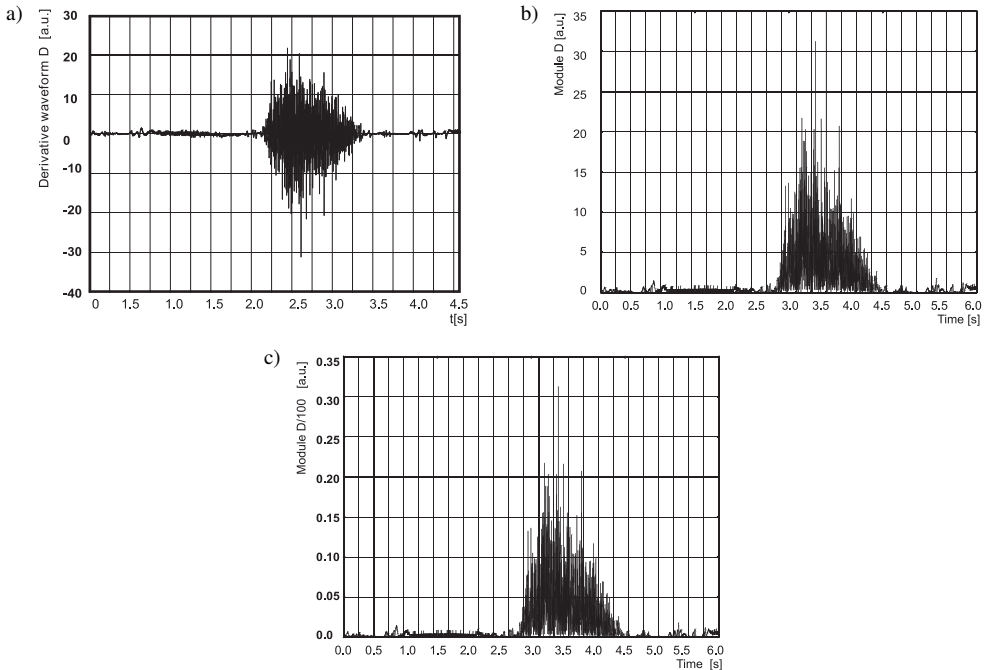

Fig. 14. Graph of the derivative of one respiratory cycle – inspiration and expiration – successively: Fig. a) – calculated derivative waveform without additional algebraic operations; Fig. b) – module of the calculated derivative; Fig. c) the value of the derivative of the tested signal after dividing by 100 (value taken arbitrarily to reconcile the axis units of the presented signal and derivative graphs). As seen from the presented graphs, rapid signal oscillations occur only during expiration in each of the presented cases. Note that the value of the derivative (related to the frequency of fluctuations) depends on the airflow rate during expiration. In the graphs, the horizontal axis of all graphs is calibrated in units of time – seconds.

www.czasopisma.pan.pl   PAN   www.journals.pan.pl
POLSKA AKADEMIA NAUK

A. Kukwa et al.: ANATOMICAL AND FUNCTIONAL ASSESSMENT OF PATENCY OF THE UPPER RESPIRATORY TRACT . . .

Figure 15 shows that the observed features of the derivative waveform of the tested respiratory flow signal allow for the determination of the times of characteristic phases in the respiration process.
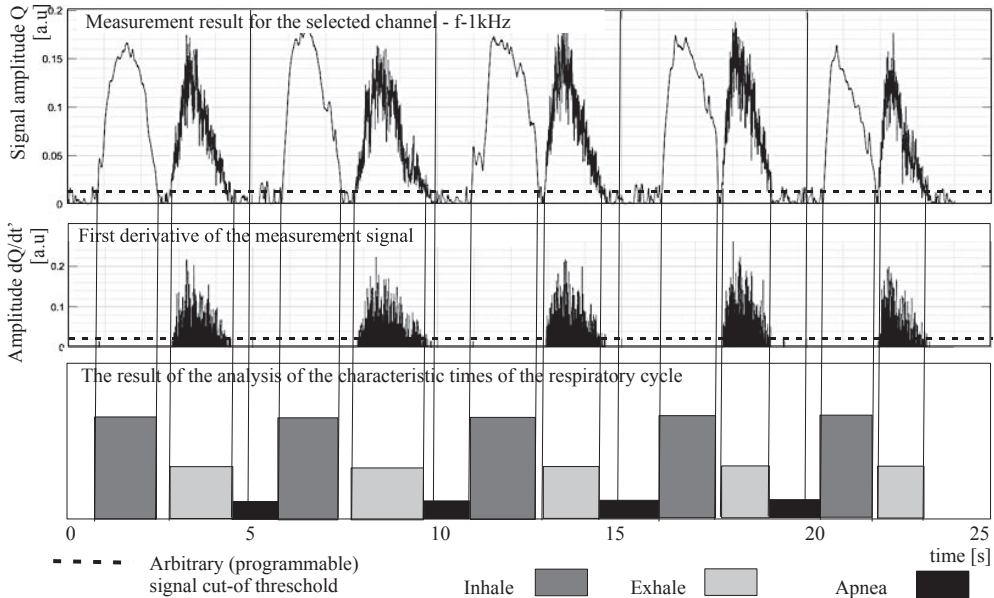

Fig. 15. Example of analysis of characteristic times in the respiration process using dedicated software.

As can be seen from the analysis of graphs and diagrams of measured respiratory parameters presented in Fig. 15, if the criterion of a non-zero derivative value (arbitrarily assumed during the analysis – blue lines on the graphs) is applied, it is possible to precisely and numerically distinguish the period of inspiration from the period of expiration.

For the next condition, the time can be determined between inspiration and expiration. Only in this order is it possible to determine the time of physiological apnoea after distinguishing between the functions of inspiration and expiration. An examplary analysis of the recorded waveform for a patient without respiratory disorders is presented in Tables 1 and 2.

Table 1. Summary of selected statistical parameters of the tested respiratory signal waveform – data as for Fig. 21, waveform selected randomly from among the tests performed.

	Inspirations	**Expirations**	**Unit**
Average inspiration/expiration duration	1.0289	0.8112	[s]
Standard deviation	0.2151	0.1541	[s]
Median	0.998	0.774	[s]
Variance	0.0463	0.0237	[s]

Figure 16 shows the panel displaying an example of statistical analysis of the conducted example examination using the developed instrument. Selected measurement cases for some disease entities are shown in the following figures.

Table 2. Summary of time parameters of the tested respiratory waveform – sample data for a pulmonologically healthy patient.

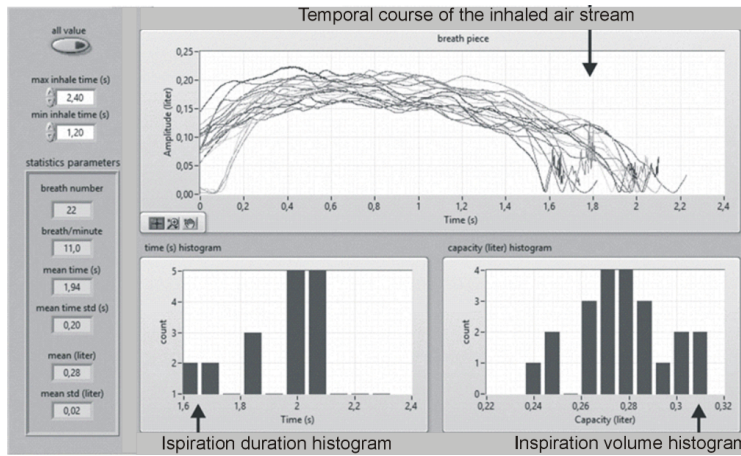|	Inspirations	Expirations	Unit
Average inspiration/expiration duration	1.0109	1.0265	[s]
Standard deviation	0.1234	0.1411	[s]
Median	1.0060	1.0565	[s]
Variance	0.0152	0.0199	[s]

Fig. 16. Example of results (for which statistical analysis can be performed) of examinations carried out using software windows developed by the authors and the device used to carry out the measurements The time waveform (airflow rate in 22 consecutive inspirations) is shown along with histograms of the inspiration time and the inspiration volume.

An analysis of the data presented in the graphs in Fig. 16 shows that the proposed diagnostic device meets many requirements for screening patients with laryngological diseases, including in-depth diagnostics of respiratory disorders during sleep.

Figure 17 presents cases of measured respiratory parameters. Sequentially from the top, Fig. 17a presents a typical waveform obtained during the measurement with the proposed method carried out in a patient without significant symptoms. In the presented graph – independently of the flow through each of the passages of the nasal cavities, a certain asymmetry appears, visible only during expiration. Since both sensors have been tested in the same conditions, and the indications differ only during expiration, there is much higher humidity of the measured medium in this phase, so it should be presumed that this factor causes the difference in the obtained results. It is also possible that two more factors affect the results obtained during expiration. The first is the time of each phase (both phases) of inspiration and expiration have different durations, and expiration is about 30% longer which causes that the flow rate during expiration is lower resulting in greater fluctuations in the anemometer readings. The second factor involves the anatomical differences and possible lesions within the nasal passages and respiratory passages (*e.g.*, the effect of drying out the mucosa in one of the passages). The graph shows smaller differences within the left passage, suggesting such an explanation.

Figure 17b shows the asymmetry of the flow through the nasal passages, resulting from anatomical differences in the structure of the nose. In the graph, the right passage has approximately 50% smaller airflow, both during inspiration and expiration.
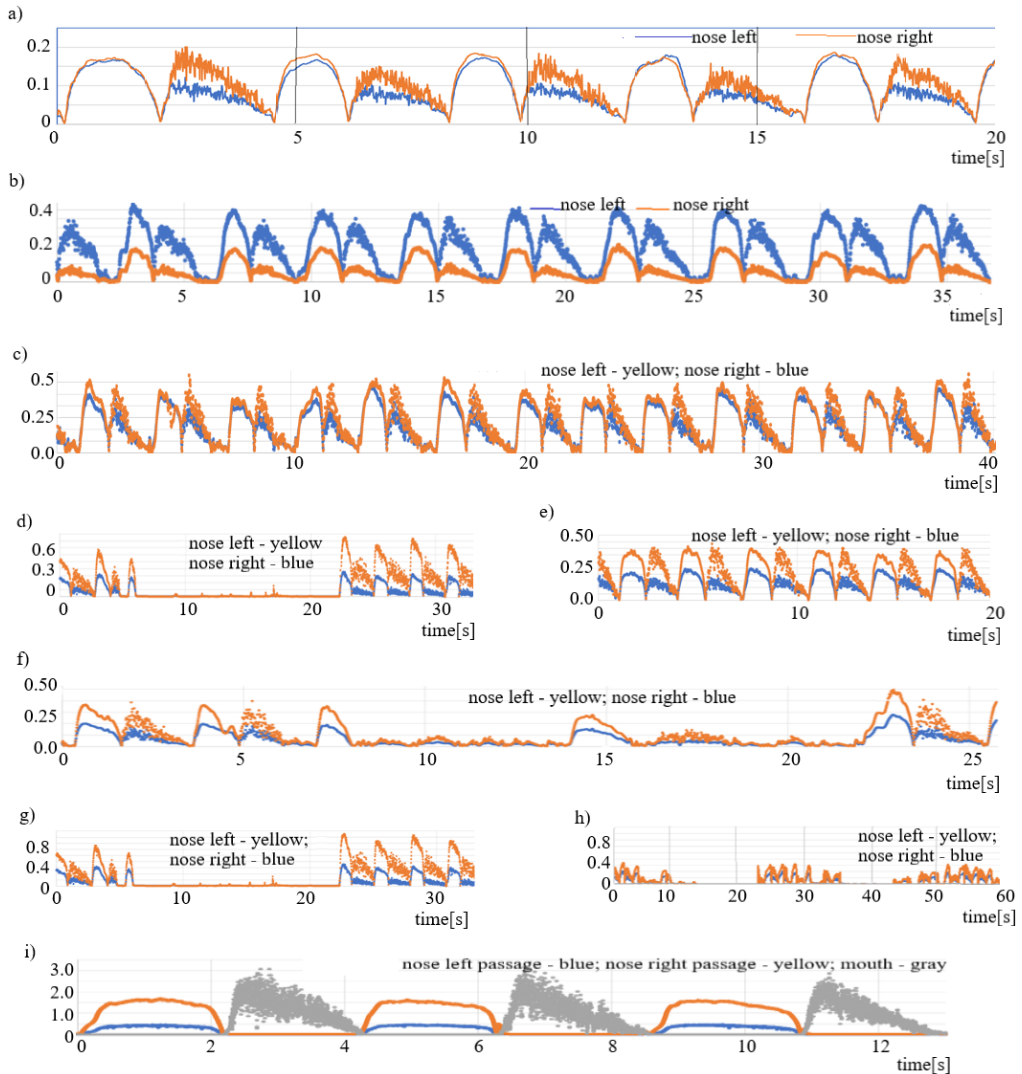
Fig. 17. Examples of registered results for selected cases. Details on the characteristics of the registered cases are discussed in the text above. On the vertical axes, in all cases, the measured value of the air flow is given. Figure: a) Correct waveform (symmetrical, a difference appears during expiration, probably resulting from different humidity – *e.g.*, dry mucosa of the right nasal passage), b) Asymmetry of the flow through the nasal passages, c), d), e) The case of a movable valve. Subsequently from the top, the patient lies on his left side, lies on his right side, in a supine position, f) A clear reduction in the respiration amplitude – a visible breathing cycle with the exchange of a small amount of air, g) Simulated apnoea, h) The case of sleep apnoea (different timescale), i) Examplary measurement using all three passages – inspiring through the nose, expiring with the mouth – extended times may result from the fact that such respiration is unnatural for the physiology of respiration.

Figure 17c shows the differences in airflows resulting from the movable valve in the nasal cavity. Although this case can be diagnosed, it is required to use a test with variable patient dynamics, *i.e.*, the patient must change his/her position during the test. As indicated in the description of the graph, tests are carried out while lying on the right or left side, and on the back.

This is neutral due to the septum geometry and functional changes depending on the patient's position.

Figure 17d presents a case of changes in ventilation time manifested by a significant reduction in inspired/expired air volume. Contrary to the case presented in Fig. 17d, temporal hypopnea in the next graph shows simulated apnoea. This waveform shows a significant increase in the volume of inspired/expired air occurring after holding breath, which allows for the reduction of the oxygen debt arising during apnoea. The last graph in Fig. 17f shows an example of flow measurement using all three measurement patterns. It is worth noting that also in the case presented in Fig. 17f the effects associated with high humidity of the expired air are manifested during expiration. Additionally, the calibration of the device can be checked and confirmed by comparing the volumes of inspired and expired air.

The automatically performed procedure for determining the duration of individual respiration phases consists in the following steps – Fig. 18. The first step selected by the operator is the possibility of scaling the device. Scaling consists of registering the waveform of respiration through selected passage, which expire specific amounts of air into a scaled tank. Such a procedure allows verifying the absolute values of the airflow rate in individual measurement passages.

The data obtained as a result of scaling makes it possible to introduce a software correction to make the obtained results real.

Scaling is necessary every few days to verify correct operation of the instrument. Performing scaling is unnecessary to test the patient's respiratory function, but it should be performed to record precise, absolute values of tidal volumes.

The patient's respiratory parameters are then measured according to the time parameters set by the medical personnel. After entering the data related to the recorded respiratory waveform, waveforms from selected sensors are saved: two nasal passages and the oral passage (only one or all three passages).

The waveforms from each of the sensors are registered independently. It is assumed that the tests related to short measurement sessions are saved in the memory of the computer operating the measuring device, while the planned tests with long testing time (several hours) are saved in the cloud, which requires storage space and a declaration when initiating the test. According to the above-mentioned procedure, detailed analyses of respiratory parameters can be preceded by an analysis using wavelet transforms [16, 17], allowing for an initial selection of some phenomena occurring during the test. Examples of the results obtained in the analysis mode are shown in Fig. 18 and 19.
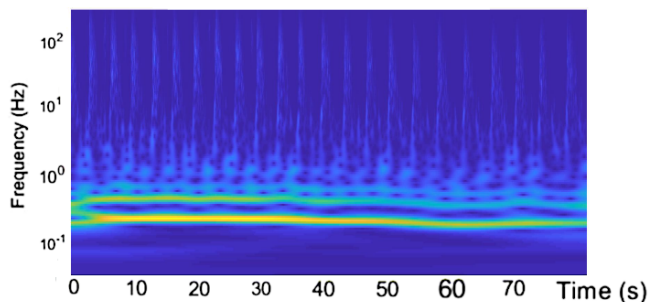

Fig. 18. Example of the result of analysis of a respiratory waveform using the Morlet wavelet. The selected 1.5-minute waveform of the respiratory cycle is included. The colours indicate the signal amplitude – yellow is the highest signal value, here the respiratory rhythm, light blue indicates the signal components with smaller amplitudes, dark blue is the picture's background.

831

www.czasopisma.pan.pl   PAN   www.journals.pan.pl
POLSKA AKADEMIA NAUK

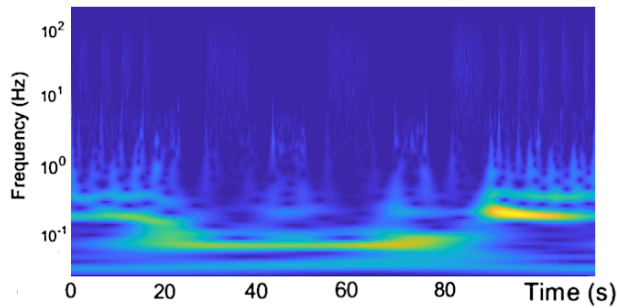A. Kukwa et al.: ANATOMICAL AND FUNCTIONAL ASSESSMENT OF PATENCY OF THE UPPER RESPIRATORY TRACT...

Fig. 19. Exemplary wavelet analysis of a respiratory waveform with noticeable disturbances, a significant reduction in respiratory rate within 20–90 seconds indicates apnoea occurring in this period. Colour markings are similar to those in Fig. 18.

The transformation presented in Fig. 18 allows for the formulation of several basic conclusions:

– The waveform presented in Fig. 18 shows the range of frequencies registered in the recorded signal in the tested signal and covers the spectrum from a fraction of Hz to approx. 1 kHz (signal sampling frequency),

– Noticeable dominant frequencies (yellow areas) are related to the recorded inspirations and expirations, with the frequency of 0.3 Hz appearing to be dominant. An earlier detailed analysis of time waveforms of the breathing process indicates that this frequency corresponds to expiration. The second area corresponding to the frequency of 0.5 Hz is the inspiration frequency. The graph shows slight, local changes in frequency in both analysed respiratory cycles.

The frequencies in the 5–100 Hz range visible in the presented waveform are related to the stochastic reaction of the thermal anemometer sensor to humidity changes in the tested flow stream.

Figure 19 shows a selected fragment of the recorded respiratory cycle containing apnoea from 20–90 seconds. During apnoea, the attenuation of frequencies related to re-modulation of the expiration waveform manifests itself in a specific manner, *i.e.*, frequencies in the range above 10 Hz

Software was developed to analyse parameters of the respiration cycle, allowing the following to be determined:

– respiration cycles divided into inspiration and expiration,
– respiration cycle frequency parameters,
– identification of selected respiratory disorders, *e.g.*, apnoea, low amplitude respiration,
– determination of quantitative parameters of the respiratory cycle,
– calculation of statistical parameters for the selected (according to specific criteria) statistical data of the measured signal.

The results of the analysis are presented using the interface shown in Fig. 20.

The Fig. 21 shows exemplary results of statistical analysis of the selected respiratory waveform.

The instrumentation developed to analyse the recorded respiratory rhythm signal (both time changes and those related to the quantitative assessment of gas exchange in the lungs) allows for a quantitative analysis of basic respiratory parameters. The instrumentation enables identifying typical disorders associated with selected diseases, including disorders difficult to diagnose using typical diagnostic techniques (in this number those for vital body functions).
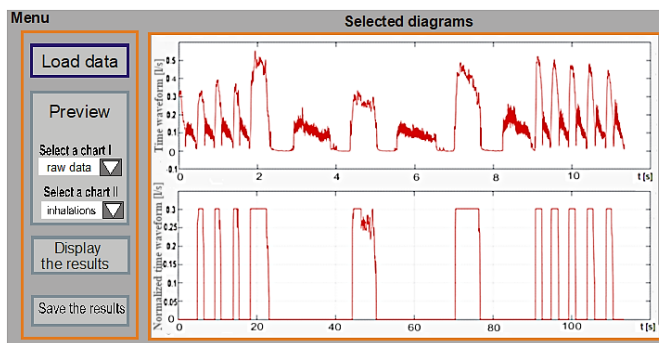
Fig. 20. View of the control panel of the developed software with an exemplary graphic visualisation of selected inspirations. The software uses the methodology described in the earlier part of the study. On the control panel the are fields initiating selected software functionalities: data input for analysis is initiated with the Load data button, the Preview area, the "Select a chart I or II" button allow users to indicate the type of data analysis, the "Displays the results button" allows users to view the obtained results – statistical data, histograms, the "Save the results button" allows users to save the test and give a name to the obtained results.
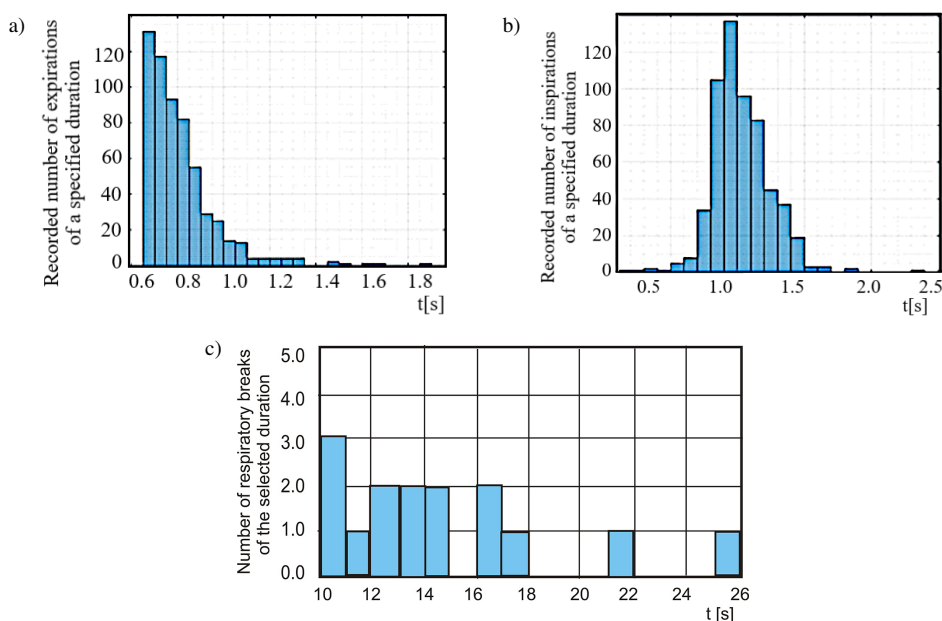

Fig. 21. Histograms showing the statistics of values of inspiration and expiration parameters in selected tests of respiratory parameters. As can be seen, the duration of the individual phases of respiration – inspiration and expiration – is not the same (two histograms in Fig. a) and b)). Fig. c) presents an exemplary histogram confirming the possibility of analysing respiratory disorders – the result for the period with apnoea – 3 apnoeas lasted about 10s (at this level, the physiological apnoea limit is defined), and one apnoea was recorded with a duration of 22s and one with 26 s.

Normally, a healthy person breathes 12–17 breaths per minute at a resting rate. The pattern of breathing is a way of respiration determined by the work of the muscles that dominate inspiration. The pattern of breathing depends on gender and health. In women, the thoracic pattern, *i.e.*, mainly based on the external intercostal muscles, is dominant. In men, the abdominal pattern,

i.e., mainly based on the diaphragm, is dominant. Figure 22 shows exemplary quantitative results for volume statistics of individual respirations.
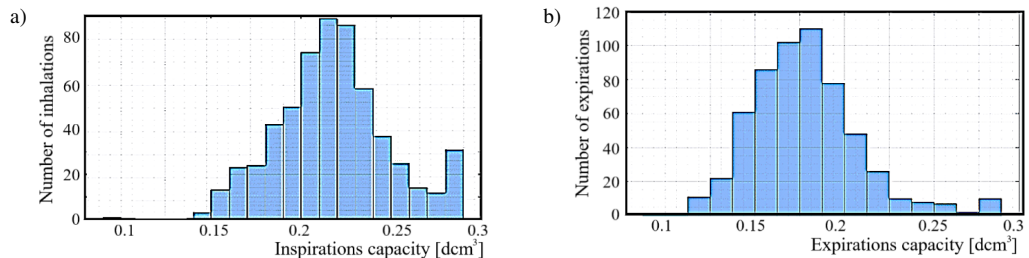

Fig. 22. Exemplary results showing the dispersion of volumetric parameters for inspirations a) and expirations b).

4. Summary

The presented article discusses selected physical diagnostic methods that can be applied in otolaryngology. A selection of diagnostic procedures and methods, mainly optical, was discussed in detail, including the existing development possibilities of the presented solutions. Each of the methods presented in the study has advantages and disadvantages, uses different physical phenomena and allows specific features of the examined lesions and pathological changes to be observed. Often, a quick and accurate diagnosis is associated with the need to conduct tests using various methods. It was also noted that in many of the indicated procedures it is possible to significantly increase diagnostics accuracy. Many elements of the procedure performed using the developed measurement methods significantly increase the speed and precision of analysis. The presented methods allow various diagnostic methods to be employed, which increases the quantity of analysed measurement data but enables finding hidden correlations that may not be visible individually in each of the methods. One of such possibilities is to study events from the standpoint of various medical specialities. The current example is the diagnosis of sleep apnoea.

Part II will discuss the properties of optical methods in medical diagnostics. Sample applications for selected disease units will be shown. Significant metrological and diagnostic features resulting from the application of the discussed methods will be indicated.

References

[1] Anniko, M., Bernal-Sprekelsen, M., Bonkowsky, V., Bradley, P. J., & Iurato, S. (2010). *Otorhinolaryngology, Head and Neck Surgery*. Berlin: Springer. https://www.doi.org/10.1007/978-3-540-68940-9

[2] Önerci, M., Ferguson, B. (2010). *Diagnosis in Otorhinolaryngology*. Berlin, Heidelberg: Springer-Verlag. https://www.doi.org/10.1007/978-3-642-11412-0

[3] Guibas, G., & Papadopoulos, N. (2017). *Viral Upper Respiratory Tract Infections. Viral Infections in Children*, *II*, 1-25. Springer, Cham. https://www.doi.org/10.1007/978-3-319-54093-1_1

[4] Kumpitsch, C., Koskinen, K., & Schöpf, V. Moissl-Eichinger, C. (2019). The microbiome of the upper respiratory tract in health and disease. *BMC Biol, 17*(87). https://doi.org/10.1186/s12915-019-0703-z

[5] DeBerry-Borowiecki, B., Kukwa, A., & Blanks, R. H. I. (1988). Cefalometric analysis for diagnosis and treatment of obstructive sleep apnea. *BMC Biol, 98*(2), 226-234. https://doi.org/10.1288/00005537-198802000-00021

[6] Jarmołowicz-Aniołkowska, N. (2020). *Private report.*

[7] Rybak, A., Zając, A., & Kukwa, A. (2019). Measurement of the upper respiratory tract aerated space volume using the results of computed tomography. *Metrology and Measurement Systems, 26*(2), 387–401. https://doi.org/10.24425/mms.2019.128366

[8] Nitkiewicz, Sz., Barański, R., Kukwa, A., & Zając, A. (2018). Respiratory disorders, measuring method and equipment. *Metrology and Measurement Systems, 25*(1), 187–202. https://doi.org/10.24425/118157

[9] Nitkiewicz, Sz. (2018). *Wspomaganie diagnostyki wybranych schorzeń dróg oddechowych* [Doctoral dissertation, Białystok University of Technology]. (in Polish).

[10] Mitchel, C. (2017). Endoscopic Examination of the Upper Respiratory Tract. In L. R. R. Costa, & M. R. Paradis (Eds.) *Manual of Clinical Procedures in the Horse* (1th ed.). John Wiley & Sons. https://doi.org/10.1002/9781118939956.ch20

[11] Zając, A., Gryko, Ł., & Gilewski, M. (2015). Temperature stabilization of the set of laser diodes working independently. *Electrical Review, 91*(2), 196–198. https://doi.org/10.15199/48.2015.02.44

[12] Zając, A., Kasprzak, J., Urbański, Ł., Gryko, Ł., Szymańska, J., & Maciejewska, M. (2016). Światło w diagnostyce medycznej. In A. Michalski (Ed.). *Metrologia w medycynie – wybrane zagadnienia.* (pp. 219-298). WAT. (in Polish)

[13] Polak, A. G., & Hantos, Z. (2019). Simulation of respiratory impedance variations during normal breathing using a morphometric model of the lung. In *World Congress on Medical Physics and Biomedical Engineering 2018* (pp. 553–557). Springer, Singapore. https://doi.org/10.1007/978-981-10-9035-6_102

[14] Polak, A. G., & Mroczka, J. (2017, May). Modeling the impact of heterogeneous airway narrowing on the spirometric curve. In *Proceedings of the 9th International Conference on Bioinformatics and Biomedical Technology* (pp. 70–75). https://doi.org/10.1145/3093293.3093301 (in Polish).

[15] Nyquist, H. (1928). Certain topics in Telegraph Transmission Theory. *Transaction of the American Institute of Electrical Engineers. 47*(2). https://doi.org/10.1109/T-AIEE.1928.5055024

[16] Bialasiewicz, J. T. (2015, July). Application of wavelet scalogram and coscalogram for analysis of biomedical signals. In *Proceedings of the World Congress on Electrical Engineering and Computer Systems and Science* (Vol. 333). Spain. https://avestia.com/EECSS2015_Proceedings/files/papers/ICBES333.pdf

[17] Daubechies, I. (1992). *Ten Lectures on Wavelets*. Society for Industrial and Applied Mathematics. https://doi.org/10.1137/1.9781611970104
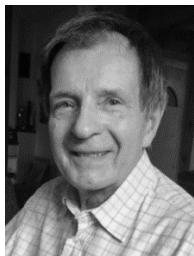
Andrzej Kukwa received his PhD degree in 1971 and obtained his DSc degree in 1974, both in Medical Science. He became Full Professor at the Medical Academy, Warsaw in 1990. He had been Head of the Otolaryngology Clinic, Department of Dentistry, Medical Academy in Warsaw from 1989 to 2011. From 2011 had been Head of the Department and Clinic of Otorhinolaryngology of Head and Neck Surgery at the University of Warmia and Mazury in Olsztyn. He has received scholarships four times in the USA. He is the author or co-author of over 200 papers, and a co-author of several patents. He has been the supervisor of 11 doctoral dissertations, tutor of 20 specializations for the 1st and 2nd degree in Otolaryngology.

Wojciech Kukwa is Professor at Medical University of Warsaw, Chief of the ENT, Head and Neck Surgery Department at Czerniakowski Hospital in Warsaw. He is a founder of the Healthy Sleep Foundation which has performed a sleep disorders screening in Polish children. Currently his research interests focus on Clebre Sleep which is a research and development project on personalized sleep diagnostics. He has published extensively including book chapters, articles and original papers in peer-reviewed journals on sleep medicine and head and neck oncology. He is a member of the Polish Society of Otorhinolaryngology, Head and Neck Surgery, the European Sleep Research Society, and the International Surgical Sleep Society.
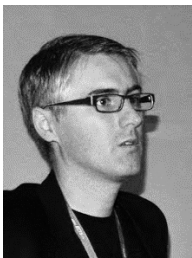
Andrzej Zając received the M.Sc. degree in Technical Physics in 1979, the Ph.D. degree in Electronics in 1987, and the DSc degree in Electronics in 1998, all from the Military University of Technology in Warsaw. From 1979 to 2021 he worked at the Institute of Optoelectronics, Military University of Technology in Warsaw, where he was engaged in the investigations of laser systems and optical measuring methods for medical applications. Since 2001 he has been Professor at the Military University of Technology in Warsaw. He is the author of more than 300 scientific publications.

Edyta Zomkowska, M.D., completed her specialization in Clinical Speech and language pathology in 2015 at the Department of Phoniatrics and Audiology of the Heliodor Święcicki Clinical Hospital at Poznań University of Medical Sciences. In 2017, she received the M.D. degree from the Faculty of Medicine at the University of Warmia and Mazury in Olsztyn. Since 2011 she has worked at the Department of Otorhinolaryngology, Head and Neck Surgery and the Clinical Department of Neurological and Systemic Rehabilitation of the University Clinical Hospital in Olsztyn. The focus of her professional work are swallowing disorders and breathing difficulties during sleep.

Robert Barański received the M.Sc. degree in Mechanical Engineering in 2002, the Ph.D. degree in Mechanics in the field of Vibroacoustics, in 2007, and the DSc. degree in Mechanics in the field of Engineering and Technical Sciences in 2019. Since 2006 he has worked at the Department of Mechanics and Vibroacoustics, AGH University, Cracow. His scientific interests focus on biomechanics, EMG signals analysis, embedded systems, diagnostic and measurement systems.

Adam Rybak received the BSC degree from Warsaw University of Technology in 2013, and the MSc degree in Electronic Engineering and Telecommunications in 2016 from Institute of Optoelectronics of the Military University of Technology in Warsaw. He is currently pursuing the Ph.D. degree there. His research activity is focused on the application of optoelectronics in medicine.

Szymon Nitkiewicz received the MSc degree in Mathematics in 2006 and the PhD in Biocybernetics and Biomedical Engineering in 2018. His experience in mathematics allows him to analyze in detail a wide range of issues. His scientific interests focus on topics related to supporting medical diagnostics and assessing the impact of human activity on the environment. He is the author and co-author of more than 20 research papers with abstracts. He owns several patents for devices which were awarded at international exhibitions.